NC STATE UNIVERSITY

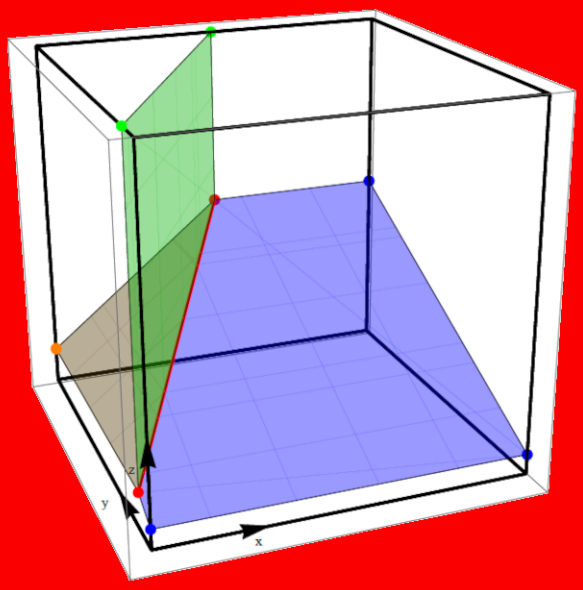

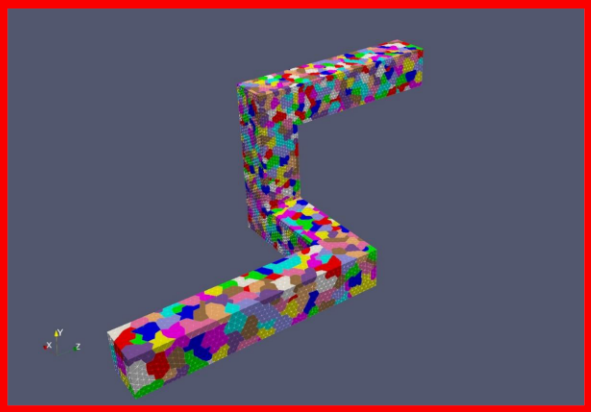

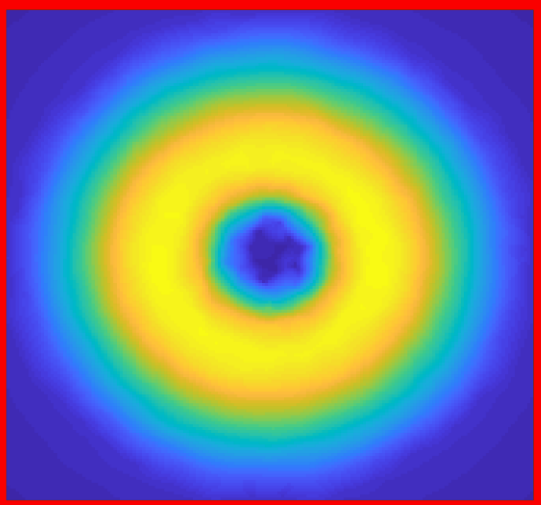

NC State University - Nuclear Computational Science Group

THOR Theory Manual

Nicholas Herring[1], Raffi Yessayan[1], Sebastian Schunert[2], Rodolfo Ferrer[3], and Yousry Azmy[1]

[1]North Carolina State University
[2]Idaho National Laboratory
[3]The Pennsylvania State University

09/07/2022

DEPARTMENT OF NUCLEAR ENGINEERING
NC STATE UNIVERSITY

NC STATE

Revision Log

Version	Date	Affected Pages	Revision Description
1.0.0	09/07/2022	All	Initial Release

Acronyms

THOR *TetraHedral-grid High Order Radiation transport code*

AHOT *Arbitrarily High Order Transport*

AHOT-C *Arbitrarily High Order Transport method of the Characteristic type*

AHOT-N *Arbitrarily High Order Transport method of the Nodal type*

AHOT-C-UG *Arbitrarily High Order Transport method of the Characteristic type on Unstructured Grids*

SN discrete ordinates

MOC *Method of Characteristics*

LC *Linear Characteristics*

SC *Step Characteristic*

DFEM *Discontinuous Finite Element Method*

DGFEM *Discontinuous Galerkin Finite Element Method*

ESC *Extended Step Characteristics*

SBA *Slice Balance Approach*

CT *Characteristic Tetrahedron*

Contents

1. Introduction

The purpose of this Theory Manual is to present a brief but complete review of the theory underlying the THOR transport code.

The THOR transport code embodies the implementation in modern Fortran of a solver for the steady state, multigroup, discrete ordinates (SN) approximation of the transport equation in three-dimensional geometry. The spatial discretization is accomplished via the *Arbitrarily High Order Transport method of the Characteristic type* (AHOT-C) [6] on tetrahedral cells [12]. For computational efficiency purposes the code solves the first-order restriction of AHOT-C, but the user is able to access the full AHOT-C code if needed. Generally, the AHOT-C formalism permits approximating the solution of the neutral-particle (neutrons and photons) transport equation through the use of a high-order short characteristics-based spatial discretization by projecting the flux within and on the faces of the tetrahedral cell onto polynomials of arbitrary order. By arbitrary order we mean an order selected by the user at run time that does not require implementation of new code for the additional higher orders. This method was developed and tested earlier in two-dimensional Cartesian geometry in a Nodal flavor (AHOT-N)[4] and the Characteristics flavor [6]. Later the AHOT-C method was extended to unstructured tetrahedral Grids (AHOT-C-UG) but numerical instabilities plagued this early version of the method. The current version of the code grew out of a Doctoral project [10] that addressed these numerical instabilities and implemented and tested its performance in the first incarnation of THOR. Since that time, several contributors over the years supported further developments, improvements, and bug fixing. The added features and the resulting publications are reviewed in the following sections of this Manual, so the citations in each section should give proper credit to the individual contributors to each feature in the code. As such, this Manual, as well as other manuals in this repository are living documents that are expected to evolve with time.

A concise historical record of THOR follows. The initial derivation and implementation of the AHOT-C-UG approach, presented in [5], revealed difficulties which were addressed in [11] and resolved in [10]. The THOR transport code originated from the work presented in [10] and, hence, the interested reader is encouraged to read that particular work if more detail regarding the basic theory and early testing of the THOR transport code is desired.

1.1 Background and Previous Work

THOR is designed to solve the steady-state, multigroup, SN approximation of the transport equation for neutral particles, namely neutrons and photons, in three-dimensional configurations. The underlying spatial discretization method is based on the method of Short Characteristics applied to tetrahedral cells comprising an unstructured mesh. The method of Short Characteristics computes the outgoing angular flux from a single cell, and the flux distribution over the cell's volume using the incoming angular flux to that cell and the source distribution over the cell's volume. The incoming flux is determined from global boundary conditions or from the outgoing flux in adjacent, upwind cells sharing the subject faces with the solved cell thus leading to the standard mesh sweep algorithm. The source distribution includes contributions from the

fixed (external) source, if specified in the problem configuration, as well as secondary-particles produced in scattering collisions, and from fission in the case of neutrons, leading to the inner/outer iteration strategy typical in neutron transport codes. The combination of mesh sweeps and inner/outer iterations, plus power iterations in criticality (eigenvalue calculations) enables solving practically any well-posed neutronics or photonics problem.

In deterministic transport codes, typically a single cell 'type' is used to approximately represent a given problem geometry and the characteristics relations are imposed exactly within each cell. Under the SN approximation, and within the scope of a single inner iteration, the mesh sweep is performed one angle at a time. For each angle, the Short Characteristics formalism is applied to cells with known incoming angular flux in a sequential order along the downwind direction of the specific angle, feeding outgoing fluxes into neighboring cells until all cells in the mesh are "solved". The kernel operation over which the method's formalism is constructed utilizes a projection of the face- and volume-moments of the angular flux and source (fixed and secondary) in a cell onto some polynomial space suitable for the applicable cell-type. This is in contrast to the method of Long Characteristics, typically referred to simply as the *Method of Characteristics* (MOC), where the entire problem configuration is traversed along selected tracks along which particle attenuation and production are accumulated.

The reduction of the problem geometry into repeating-type, even if not identical-shape/dimensions, computational cells of a particular geometry makes it possible to treat each cell/angle pair semi-analytically. The "analytical" aspect follows from the application of the integral form of the transport equation over the cell's volume, while the "semi" aspect follows from the stated projection of the angular flux and source distributions. Solution of the transport equation's integral form using characteristics is a standard staple in introductory transport theory coursework and textbooks [16]. In the context of the method of Short Characteristics, the resulting kernel operation is comprised of evaluating the outgoing angular flux moments using the characteristics relationships on the projection basis. This is followed by enforcing the balance over the cell of each spatial moment in the employed basis using the known incoming and just-computed outgoing angular flux moments and moments of the known source moments, to compute the cell-moments of the angular flux [19].

The polynomial order of the expansion basis utilized by the method of Short Characteristics, p, influences the solution accuracy. However, a more influential factor affecting the accuracy of the method's solution is regularity of the exact solution, noting that for all known applications of the transport equation in neutronics and photonics either the exact solution or its first derivative is discontinuous in the spatial variable depending on the global boundary condition's continuity at the incoming "corners" [9]. For problems with very little scattering and unequal angular flux on incoming faces, discontinuities of the angular flux or its spatial derivatives along the outgoing faces of computational cells intersected by singular characteristics are expected to occur. Thus, the use of a continuous polynomial basis will only approximately capture the true shape of the angular flux over such cells' faces.

Three important issues concerning Short Characteristics methods are flux positivity and solution accuracy, as noted by Lathrop [15], and the asymptotic behavior of the discretization in thick diffusive problems. The first two issues are tied to the order p of the polynomial basis functions used to represent the angular flux over the cells' faces and volume. Most of the early Short Characteristics methods relied on either a flat or linear flux representation of the flux spatial profile. The constant or flat flux representation on the face and volume of a computational cell, also known as the *Step Characteristic* (SC) method, has been shown to yield a positive angular flux for positive incoming angular flux and distributed source. However, the Short Characteristics method has also been shown to be only first order accurate, thus solution positivity comes at the expense of accuracy. On the other hand, the *Linear Characteristics* (LC) method, as proposed by Larsen and Alcouffe in two- dimensions [14], is not positive definite but can achieve second order accuracy with respect to mesh refinement. Finally, the behavior of discretizations based on general-order Short Characteristics methods in thick diffusive regimes has been the topic of an asymptotic analysis reported by Adams *et al* [2]. This analysis revealed that Short Characteristics methods behave almost exactly like DFEMs in diffusive problems, and thus possess two classes of discretizations: those which fail on thick diffusive problems, and those that correctly limit to a discretized diffusion equation. The investigators proposed a family of reduced-order

Short Characteristics methods which use less information on cell surfaces, and thus behave more robustly in the thick diffusive regime.

A metrics-based study in the context of a simple two-dimensional test problem configuration considered various desired features in the numerical solution to the transport equation based on the *Arbitrarily High Order Transport* (AHOT) class of methods of the Nodal (*Arbitrarily High Order Transport method of the Nodal type* (AHOT-N)) and Characteristics (AHOT-C) types [6]. This study showed improving solution accuracy with rising local expansion order, specifically concluding that AHOT-N provides more accurate scalar flux values while AHOT-C computes more accurate current values, with the difference in accuracy level diminishing with increasing expansion order. Furthermore, that study established that even-order local expansion methods are less likely to produce negative values for the scalar flux. Note that AHOT-C of order 0 is equivalent to the SC methods that is positive. More recently, a wider collection of numerical methods employed in solving the transport equation, including AHOT-N and *Discontinuous Galerkin Finite Element Method* (DGFEM) both up to third order local expansions, among other methods, were applied to a three-dimensional, Method of Manufacture Solutions (MMS) configuration [20]. Availability of the true, MMS solution enabled quantification of the true error for each tested method *vs* various physical and numerical parameters. That study concluded that under discrete L_p norms for configurations with a continuous exact angular flux, high-order AHOT-N methods perform best, i.e. produce the most accurate numerical solution. By applying an integral error norm to the same collection of numerical solutions it was found that the Linear Nodal method (as simplification of the AHOT-N method of first order [3]) performs the best. In configurations where the exact angular flux suffers discontinuities, e.g. in certain shielding applications, the Singular Characteristic Tracking algorithm was found to perform best as it avoided smearing the incoming angular flux across the discontinuity that affects cells intersected by the singular characteristic by explicitly accounting for the location of these discontinuities [9].

1.2 Low-Order Spatial Approximations

The use of constant or linear basis functions to represent the cell-face and cell-volume based variables constitute what is considered in this section to be the low-order spatial approximations within the family of Short Characteristics methods. The constant or SC method is the earliest proposed method in which the streaming-plus-collision operator of the transport equation is formally inverted and the 'characteristic' formula is used to locally solve the transport equation. Issues of positivity and accuracy regarding the Step and LC method in two-dimensional geometry were investigated by Lathrop [15]. While higher-order methods are suggested in Lathrop's work, it is Larsen and Alcouffe [14] that introduce the LC method in two-dimensional Cartesian geometry, and later generalized to arbitrarily high order by Azmy [6]. Numerical results reported in [14] show that for shielding and deep-penetration problems, the LC outperformed the DD method with respect to solution accuracy for both fine and coarse-mesh sizes. The acceleration of the inner iterations through the application of DSA is also presented by Larsen and Alcouffe in the same paper. Results and conclusions from the study reported in [6] are summarized above.

While much of the initial theoretical and numerical development of the SC and LC methods was performed in two-dimensional Cartesian geometry, the Short Characteristics approach has gained attention as an approach that can provide numerical solutions to the transport equation in general geometries. In fact, the so-called *Extended Step Characteristics* (ESC) method developed by DeHart *et al.* [8], is an LC method for two-dimensional arbitrarily-shaped cells. The basic ESC approach is to overlay an unstructured grid on an exact solid body geometric description of the domain, which gives rise to an arbitrarily connected polygonal grid in which the LC-based method can be applied by splitting or 'slicing' each cell. Thus, the arbitrarily-connected polygonal cells can be reduced to arbitrary triangles and/or quadrilaterals, each having a single incoming and a single outgoing face per discrete ordinate. Once all face fluxes are computed, based on incoming fluxes either from neighboring cells or external boundary conditions, the interior cell angular flux is computed by imposing the balance equation over the arbitrary polygonal cell. The *Slice Balance Approach* (SBA), developed by Grove [13], is a Short Characteristic-based discretization which can handle unstructured polyhedral meshes

in a similar manner as the ESC but in three-dimensional geometry.

The Short Characteristics method has also been extended to other unstructured grid geometries, such as arbitrary triangles in two-dimensional geometry, as shown by Miller *et al* [18]. Similar to the ESC method discussed above, the LC method is used to split triangles into sub-triangles defined by the characteristic direction that is being considered, thus solving for the outgoing cell-face angular fluxes based on the sub-cell face angular fluxes and imposing a total balance over the triangular cell. The LC method has also been extended by Mathews *et al.* [17] to unstructured tetrahedral grids by applying the same approach as with unstructured triangular geometry in the plane. Finally, Brennan *et al.* [7] presented a similar split-cell characteristic approach, but expanding the cell face and interior angular fluxes into non-linear exponential basis functions. While these Short Characteristics methods have extended the LC methodology to unstructured grids, very little work has been performed in applying high-order spatial approximations to the face and interior cell angular fluxes. Thus, in the next section high-order spatial approximations are discussed in the context of the Short Characteristics method.

1.3 High-Order Spatial Approximations

First introduced by Azmy [6], the Arbitrarily High-Order Transport Characteristic (AHOT-C) method can be considered a generalization of the SC and LC methods into a general-order class of Short Characteristics methods which use a polynomial basis function for the cell-face and cell-volume angular fluxes. While the first high-order, multi-dimensional transport method was suggested by Lathrop [15], it was in the context of nodal methods that consistent high-order methods were first conceived [6] for structured Cartesian cells. By performing the moment-based transverse-averaging of the transport equation locally in a cell, a dimensionally-reduced equation could be solved 'analytically' for each coordinate direction separately. The solutions in the separate one-dimensional versions are coupled together via the leakage terms that are themselves represented as a local expansion on the cell-faces. All so-computed moments, within and on the faces of a cell, are subsequently used to perform a consistent balance over the cell's volume for all considered spatial moments. The introduction of the AHOT-N method, cast into a Weighted Diamond Difference form by Azmy [4], served as a motivation for developing an AHOT-C. While consistent spatial moments are taken over the cell to apply the balance in both AHOT-N and AHOT-C, it is the latter that solves for the outgoing angular flux moments evaluated at the cell edges by applying a Short Characteristics approach. Unlike the traditional SC and LC methods, the AHOT-C assumes a polynomial cross-product basis function in two-dimensional structured Cartesian cells. A numerical comparison between AHOT-N and AHOT-C has also been presented for a set of benchmark problems by Azmy [6], which concludes that for deep-penetration or shielding problems the AHOT-C methodology is more accurate with respect to quantities such as leakage. On the other hand, for 'neutron conserving systems', the AHOT-N methodology is found to be more accurate in terms of integral quantities, such as reaction rates.

An early extension of the AHOT-C formalism to unstructured tetrahedral grids, referred to as AHOT-C-UG, was presented in [5]. While numerical difficulties were encountered for optically thin cells and high-order spatial expansions beyond the lowest order of polynomial expansion, their first attempt to extend AHOT-C to unstructured grids remains an important step in the generalization of Short Characteristics methods. The methodology presented in this manual, that forms the foundation for the THOR transport code, is based on a reformulation of AHOT-C-UG presented in [10]. This reformulation allowed the THOR transport code to avoid previously observed numerical difficulties, hence it can be applied to realistic radiation transport problems.

2. AHOT-C-UG Theory

Let $\mathcal{D}$ denote a convex open set in $\mathbb{R}^3$ with boundary Γ and $\hat{n}$ a unit vector normal to Γ and pointing outwards of $\mathcal{D}$. The neutral-particle direction of motion is defined as the unit vector $\hat{\Omega}$ on the unit sphere $\mathcal{S} = \{\hat{\Omega} \in \mathbb{R}^3 : |\hat{\Omega}| = 1\}$. The incoming and outgoing boundaries are defined with respect to $\hat{\Omega}$ and the position vector $\vec{r}$ as subsets of the boundary Γ in the following manner, respectively:

$$\Gamma^-(\hat{\Omega}) = \{\hat{r} \in \Gamma : \hat{\Omega} \cdot \hat{n}(\vec{r}) < 0\} \tag{2.1}$$

$$\Gamma^+(\hat{\Omega}) = \{\hat{r} \in \Gamma : \hat{\Omega} \cdot \hat{n}(\vec{r}) > 0\} \tag{2.2}$$

Given the above definitions it is now possible to define the following boundary value problem: find the angular flux $\psi(\vec{r}, \hat{\Omega})$ that satisfies the steady-state, one-speed transport equation

$$\hat{\Omega} \cdot \nabla\psi(\vec{r}, \hat{\Omega}) + \sigma_T(\vec{r})\psi(\vec{r}, \hat{\Omega}) = \frac{\sigma_s(\vec{r})}{4\pi}\Phi(\vec{r}) + q(\vec{r}). \tag{2.3}$$

In Eq. 2.3 we assumed a non-multiplying medium with isotropic scattering, but these constraints are easy to relax. Indeed the current version of THOR is capable of modeling transport phenomena in multiplying media with anisotropic scattering. Equation 2.3 is supplemented with applicable boundary conditions of the standard form

$$\psi(\vec{r}, \hat{\Omega}) = \psi_{bc}(\hat{\Omega}), \vec{r} \in \Gamma^-(\hat{\Omega}) \tag{2.4}$$

where the total and scattering macroscopic cross-sections, σ_T and σ_s, are assumed to be positive and constant across a material region such that the scattering ratio $c = \sigma_s/\sigma_T$ remains smaller than unity. The *scalar* flux is defined in terms of the angular flux such that

$$\Phi(\vec{r}) = \int_{4\pi} d\hat{\Omega}\psi(\vec{r}, \hat{\Omega}) \tag{2.5}$$

where the integral over $\hat{\Omega}$ represents the contribution of the angular flux over all possible directions. The fixed source $q(\vec{r})$ represents the contribution to the angular flux from particles emitted by the external source that implicitly include in the case of a multiplying media, contributions from fission events.

Two important assumptions regarding the model problem presented above. First, the scattering from a given direction $\hat{\Omega}'$ into another direction $\hat{\Omega}$ was assumed to be isotropic, implying an equal probability for particles emitted in a scattering event to appear in any direction. However, THOR accounts for anisotropic

scattering in the standard fashion of expanding the scattering cross section's angular dependence in Legendre polynomials then using Legendre's Addition Theorem to write the angle-dependent scattering source in terms of angular moments of the flux. These details are skipped here but are available to the novice reader in standard textbooks if needed [16]. Second, the model as written assumes that the flux has no energy dependence. The addition of energy dependence to the angular flux, also known as the multi-group method, is usually formulated by simply assuming that Eq. 2.3 holds for each pre-defined energy group and group-dependent macroscopic cross-sections, thus producing a coupled set of equations for each energy group. This aspect is treated in THOR using the traditional inner/outer iteration strategy, and we focus the current development of the AHOT-C-UG methodology on the simplified model for simplicity, but without any loss of generality.

Next, the discrete-ordinates approximation is introduced by applying Eq. 2.3 to a pre-selected set of angles $\hat{\Omega} = (\mu_1, \mu_2, \mu_3)$, where μ_1, μ_2, and μ_3, are angle-cosines of the vector $\hat{\Omega}$ with respect to the global orthogonal coordinate system's x, y, and z axes, respectively. The discrete-ordinates, or S_N, method requires Eq. 2.3 to be solved for a set of $M(N)$ discrete directions $\{\hat{\Omega}_n\}$ associated, per individual angle, to a set of quadrature weights $\{\omega_n\}$ such that the scalar flux definition, Eq. 2.5, is approximated by

$$\phi(\vec{r}) \approx \sum_{n=1}^{M(N)} \omega_n \psi_n(\vec{r}) \tag{2.6}$$

where the S_N angular flux approximates the angular flux along directions $\hat{\Omega}_n$, i.e. $\psi_n(\vec{r}) \approx \psi(\vec{r}, \hat{\Omega}_n)$, and the quadrature weights ω_n are normalized by $\sum_{n=1}^{M(N)} \omega_n = 4\pi$. Thus, the S_N approximation to the steady-state, mono-energetic transport equation is obtained

$$\hat{\Omega}_n \cdot \nabla \psi_n(\vec{r}) + \sigma_T(\vec{r}) \psi_n(\vec{r}) = \frac{\sigma_s(\vec{r})}{4\pi} \sum_{m=1}^{M(N)} \omega_m \psi_m(\vec{r}) + q_n(\vec{r}), n = 1, ..., M(N) \tag{2.7}$$

with the S_N boundary conditions

$$\psi_n(\vec{r}) = \psi_{bc,n}, \vec{r} \in \Gamma^-(\hat{\Omega}_n) \tag{2.8}$$

In order to lighten the notation, the scattering and external sources will be combined into a single term to define a *total* source $Q_n(\vec{r})$, and by assuming that the fixed source is isotropic, we can write $Q(\vec{r}) = Q_n(\vec{r})$ in the ensuing presentation, without any loss of generality.

2.1 Transformation Among Global, Cell, and CT Coordinate Systems

Unlike the case of AHOT-C, in which the computational cell boundaries coincide with a global Cartesian coordinate systems, THOR's tetrahedral mesh precludes such alignment. The AHOT-C-UG formalism is greatly simplified via the transformation of an arbitrary tetrahedral cell into a unit tetrahedral cell. This transformation simplifies the derivation of the final set of discrete-variable equations and allows for a single series finite expansion of the 'characteristic kernel', i.e. integral term of the characteristic relation along the streaming direction. The transformation of an arbitrary tetrahedron, and subsequent integration of functions over its volume, has been successfully applied to the development of a LC method for tetrahedral grids [17]. In order to apply the necessary transformations to the AHOT-C-UG approach, an analogous approach to the transformations presented in [17] was developed. In summary, all transformations of the cells and

Characteristic Tetrahedra (CTs), to be defined shortly, into local face- and volume-coordinate systems are performed numerically through the use of Jacobian matrices and utilizing their determinants. Thus, an incoming angular flux in the direction of motion $\hat{\Omega}$ may be transformed into a local CT volume-coordinate system and the corresponding outgoing angular flux computed through the use of a local characteristic relation.

2.1.1 Standard *Characteristic Tetrahedron* (CT) Configuration

The CT configuration defines the splitting or slicing of an arbitrary tetrahedral cell into constituent CTs with respect to a discrete angular direction $\vec{\Omega}$. More specifically, an arbitrary tetrahedron may be split into CTs depending on the number of incoming and outgoing cell faces of the original tetrahedron with respect to the particle direction of motion. The total number of potential configurations depends on the cell's orientation relative to $\vec{\Omega}$. The resulting CTs share an edge that parallels the subject $\vec{\Omega}$; hence each CT, by definition, possesses exactly one incoming face, exactly one outgoing face, and two faces across which no particles flying along $\vec{\Omega}$ can flow. The benefit of this strategy is that it allows the development of the AHOT-C-UG formalism and discrete variable equations for a single CT configuration, solving these locally, then combining the contribution of constituent CTs to the edge- and cell-fluxes to compute the corresponding values for the original tetrahedron.

For a particular instance of an arbitrary tetrahedron, three standard CT configurations are possible: one incoming face and three outgoing faces, two incoming and two outgoing faces, and three incoming faces and one outgoing face as sketched in 2.1.

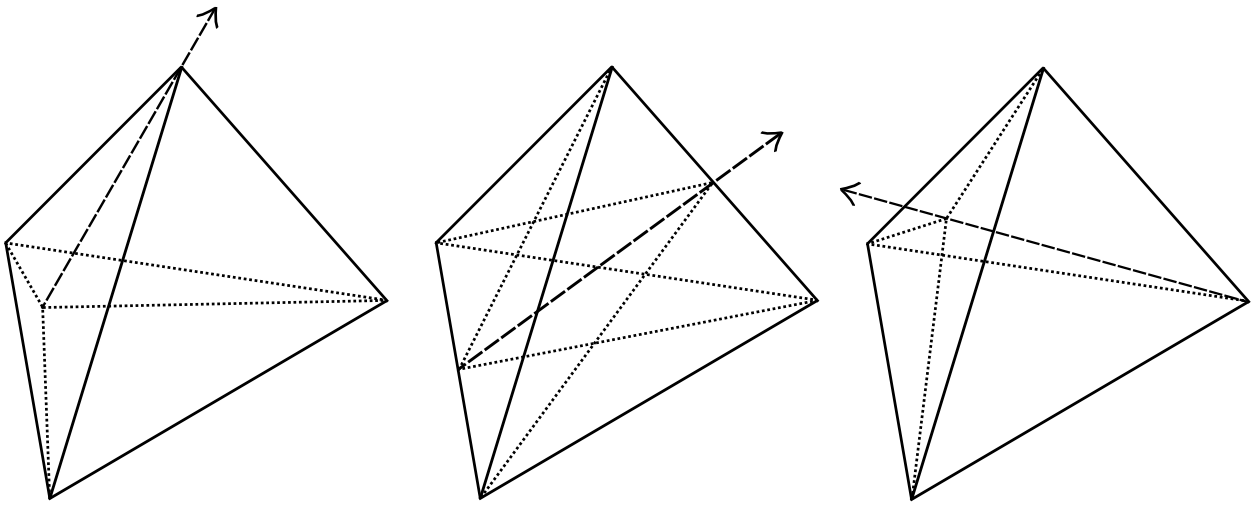

Figure 2.1: Potential *Characteristic Tetrahedron* (CT) configurations for non-planar angular direction.

The first standard configuration involves a single incoming face and three outgoing faces with respect to the angular direction of the particle flow. To apply the AHOT-C-UG formalism to this tetrahedron, we split it into three CTs, thus allowing the computation of the angular flux over each CT and its outgoing face via the short characteristics equations.

The second standard configuration involves two incoming faces and two out-going faces with respect to the angular direction. Unlike the previous standard configuration, it is necessary to determine both incoming and outgoing position vectors, in order to split the tetrahedron. These vectors, analogous to the first standard configuration, are defined with respect to the global coordinate system. In order to determine the characteristic length τ, the arbitrary tetrahedron can be mapped into a normalized tetrahedron and the characteristic length can be determined based on the local angular direction.

The determination of the characteristic length involves the selection of a particular set of equations from the set of equations relating the global and local coordinate systems. The local coordinate system can provide the specific values that are needed to determine the characteristic length. In order to derive the formulas for τ, it is necessary to consider every potential case in the normalized coordinate system.

The final standard configuration involves three incoming faces and a single outgoing face with respect to the angular direction. In order to split such tetrahedron into CTs, it is necessary to determine the incoming position vector. It is worth noting that this particular case is identical to the standard configuration 1 with the "in" and "out" designations for the corresponding position vectors interchanged.

In the event that the particle flight direction, $\vec{\Omega}$, is co-planar with one of the original tetrahedron's faces, or coincident with one of its edges the resulting set of potential CT splits is illustrated in 2.2.

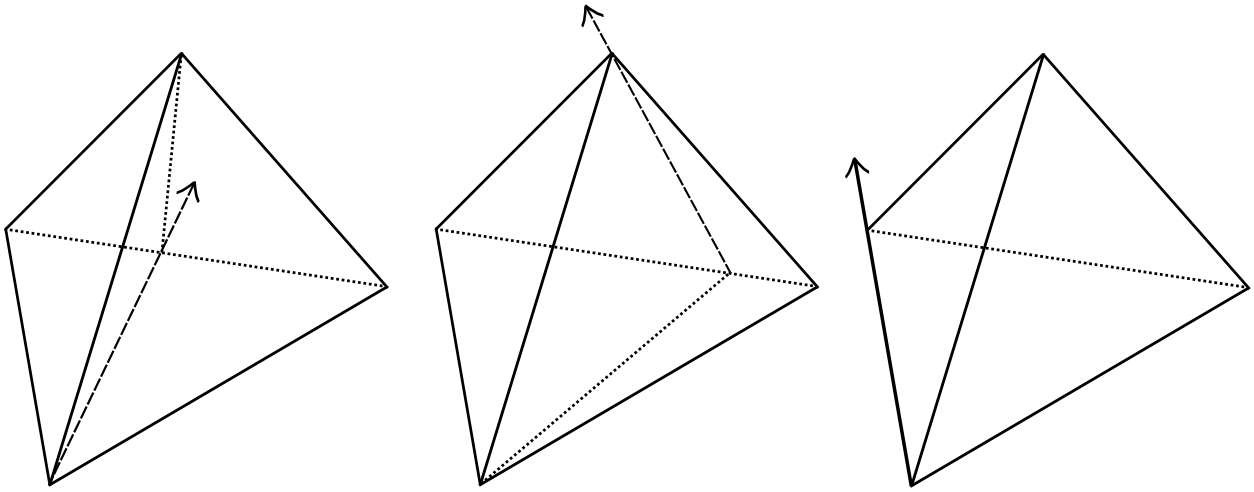

Figure 2.2: Simplified *Characteristic Tetrahedron* (CT) configurations for planar coincidental angular direction.

The first simplified configuration involves two incoming faces and a single outgoing face with respect to the angular direction. To split the cell, it is necessary to determine the outgoing position vector, which is the projection of the incoming vertex along the local angular direction to the outgoing face. It is worthwhile to note that this particular case is identical to the standard configuration 2 with two instead of three constituent CTs.

The second simplified configuration involves one incoming face and two out-going faces with respect to the angular direction. In order to split the cell into CTs, it is necessary to determine the incoming position vector, which is the projection of the outgoing vertex backwards along the angular direction to the incoming face.

The third simplified configuration involves a single incoming face and a single outgoing face. This particular case occurs when the angular direction $\vec{\Omega}$ is parallel to exactly one edge of the arbitrary tetrahedron. In this case, the arbitrary tetrahedron reduces to a CT and as such, it does not require any splitting. This simplified configuration rarely occurs in actual applications, since the generation of the mesh and the selection of the angular quadrature are performed independently. However, this configuration is also particularly important due to the fact that the discrete-ordinates solution being approximated by the AHOT-C-UG over the discrete mesh will be smooth, since all potential discontinuities or so-called 'singular characteristics' [9] will lie along the no-flow faces of the subject tetrahedrons, and thus they make no contribution to the incoming and outgoing angular fluxes over a given cell. This feature of the discrete problem, in which high-order convergence may be observed, is attained provided that the tetrahedral grid is constructed in such a way that every cell has at least one side that is parallel to the particle flow angular direction. This type of mesh generation strategy is termed "aligned mesh".

With regards to implementation into THOR, an algorithm that determines the applicable CT configurations with respect to a given cell's orientation is devised by simply testing the number of incoming and outgoing cell faces. Since the unstructured nature of the geometric description makes it impossible to determine *a priori* the sweeping order of the mesh in the context of a single inner iteration, each cell is examined throughout the mesh-sweep process to determine the applicable CT configuration. This enables locally solving the moments-balance and Short Characteristics equations simultaneously for each resulting CT, then the computed values are combined into face- and cell-moments of the angular flux valid for the original tetrahedral cell. Hence, the information regarding the number of incoming and outgoing faces is determined on the fly and need not be stored, thus relieving the memory storage burden.

2.2 The AHOT-C-UG Formulation

The AHOT-C formulation in two-dimensional Cartesian geometry [6] involved the derivation of two fundamental sets of equations for each cell:

1. The arbitrary-order balance equation over the cell, that relates the angular flux face-moments and distributed source cell-moments to the cell-moments of the angular flux.
2. The arbitrary-order characteristic relation, that relates the angular flux incoming face-moments and distributed source cell-moments to the angular flux outgoing face-moments.

An analogous approach is adopted in AHOT-C-UG, except for the fact that the quantities of interest are defined in a transformed local coordinate system that does not leave the discrete-variable transport operators invariant, and as such requires a sequence of transformations in order to obtain discrete-variable expressions for the face- and cell-moments of the angular flux. These transformation procedures allow for the expansion of the angular flux and the source to be represented in the local cell and CT coordinate system, thus simplifying the final set of equations that are implemented in THOR. It is important to note that none of these transformations introduce any additional approximation to the AHOT-C-UG approach. In order to develop these transformations, first it is necessary to define the face- and cell-moments and their accompanying basis functions.

2.2.1 Polynomial Basis Function Expansion

Let $B_{\vec{i}}(\vec{r})$ denote a polynomial basis function of order $\vec{i} = \{i_j, j = 1, 2, 3\}$, where the i_j satisfy the conditions $0 \leq i_1 + i_2 + i_3 \leq \Lambda'$ if a 'complete' basis is used or the conditions $0 \leq i_j \leq \Lambda, j = 1, 2, 3$ if a 'double' Pascal tetrahedron is used, in which case all mixed (or cross) moments that satisfy the corresponding conditions are retained by the expansion. In both cases, Λ, and Λ' denote the highest order of the polynomial basis, and thus determines the spatial expansion order of the method. The basis functions for AHOT-C-UG in the cell coordinate system is the monomial basis

$$B_{\vec{i}}(\vec{u}) = u_1^{i_1} u_2^{i_2} u_3^{i_3} \tag{2.9}$$

and, similarly, in the cell-face coordinate system the basis function is the monomial

$$B_{\vec{i}^F}(\vec{u}^F) = (u_1^F)^{i_1^F} (u_2^F)^{i_2^F} \tag{2.10}$$

In general, the cell-moments in the global coordinate system are defined by

$$G_{\vec{i}} \equiv \frac{1}{V} \int_V dV B_{\vec{i}}(\vec{r}) g(\vec{r}) \tag{2.11}$$

where $g(\vec{r}) = \psi_n(\vec{r}), \phi(\vec{r})$, or $S(\vec{r})$, and V is the cell volume. The cell face- or area-moments in the global coordinate system are defined in a similar manner

$$G^F_{\vec{i}} \equiv \frac{1}{A^F} \int_{A^F} dA^F B_{\vec{i}^F}(\vec{r}^F) g(\vec{r}^F) \tag{2.12}$$

where A^F is the area of the subject cell face. The integrals in the global coordinate system are better evaluated in the cell coordinate system in order to avoid large values of the spatial-variable arguments in the former that might lead to poor numerical precision in the computed quantities. Unlike the case of orthogonal functions in structured geometries, in which basis functions such as Legendre polynomials are used in rectangular cells, the use of monomials requires the solution of a linear system of equations in order to obtain the expansion coefficients of the projected functions. Note that using orthogonal bases in unstructured grids is futile since there is no expectation of orthogonality in these configurations. For instance, if the function $g(\vec{r})$ in Eq. 2.11 is expanded locally into the set of basis functions defined in Eq. 2.9

$$g(\vec{u}) = \sum_{\vec{i}=0}^{\Lambda} g_{\vec{i}} B_{\vec{i}}(\vec{u}) \tag{2.13}$$

then the vector $\mathbf{G}$ whose $\vec{i}^{th}$ element is given by Eq. 2.11, and packing the scalar expansion coefficients $g_{\vec{i}}$ into the vector $\mathbf{g}$ we can relate these two vectors by taking the $\vec{i}^{th}$ moment of Eq. 2.13 via,

$$\mathbf{G} = \boldsymbol{M}\mathbf{g} \tag{2.14}$$

In Eq. 2.14 matrix $\boldsymbol{M}$ is the tensor product of the monomial basis (also known as the mass matrix in finite element methods), that is defined in the following manner

$$\boldsymbol{M} \equiv 6 \int_0^1 du_1 \int_0^{u_1} du_2 \int_0^{u_2} du_3 B_{\vec{i}} B_{\vec{i}}^{\boldsymbol{T}} \tag{2.15}$$

where $\boldsymbol{M}$ and $B_{\vec{i}} B_{\vec{i}}^{\boldsymbol{T}}$ are matrices of order Λ or Λ', for double Pascal or complete basis, respectively, and the superscript $\boldsymbol{T}$ denotes the transposed vector. In Eq. 2.14 the components of $\mathbf{g}$ represent the known or unknown local expansion coefficients of the function $g(\vec{r})$ if g is the fixed source or the angular flux, respectively.

The choice of monomials as basis functions was motivated by previous experience, namely the formulation of AHOT-C-UG presented in [5] that used this basis, as well as simplicity since in this basis the coordinate transformations become relatively straightforward to generalize to an arbitrary expansion order. In addition, the overall results of early investigations reported in [10] illustrated insensitivity of the computed results to the particular choice of a different polynomial basis, such as a hierarchical basis [21], as long as the basis spans the same exact function space [1]. While the structured grid-based formulation of AHOT-C used Legendre polynomials as basis functions, which retained mixed product terms, this is not generally a requirement. Due to the generality of the AHOT-C-UG formalism, it is possible to experiment with both types of basis function expansions.

The use of a 'mixed' or incomplete basis expansion introduces an additional complication that is not encountered in the case of a complete basis. This additional complication stems from the fact that, given a

particular incoming and outgoing direction in the cell coordinate system, the evaluation of the angular flux moments over the CT volume and outgoing face in the CT coordinate system must be consistent with the expansion in the cell coordinate system. For example, consider the $\Lambda = 1$ expansion, $\{1, x, y, z, xy, xz, yz, xyz\}$, over a normalized tetrahedron. Let $x = u_1, y = u_2$, and $z = u_3$ and consider the case in which the outgoing angular flux, determined by the local angular direction, exits the face defined by $u_3 = 0$, as represented by the CT located inside the first tetrahedron on the left in Fig. 2.1. The basis functions used to represent the angular flux in the cell coordinate system over the outgoing face become $\{1, x, y, xy\}$. If the incoming angular flux moments and distributed source are simply transformed to the local CT coordinate system based on an incomplete expansion, such as $\{1, x, y, z, xy, xz, yz, xyz\}$ under the assumption that $x = q_1, y = q_2$, and $z = q_3$, then the outgoing face-moments computed by the CT will automatically assume, by convention, that the outgoing angular flux exists the face defined by $u_3 = u_2$, and thus assumes that the basis expansion over the outgoing CT face is given by $\{1, x, y, xy, y^2, xy^2\}$, which is clearly different from in the cell coordinate system.

In order to maintain the correct orientation, the computation of the spatial moments of the angular flux over the outgoing face and volume has to be performed in tandem with the coordinate transformation. This peculiarity does not arise in a complete expansion, since in the case of $\Lambda' = 1$ the expansion is $\{1, x, y, z\}$ which, when evaluated over the outgoing face in the cell coordinate system is $\{1, x, y\}$, and in the CT coordinate system is $\{1, x, y\}$, both of which are clearly compatible with each other.

2.2.2 Transformation of Cell to CT Source Distribution

In order to simplify the computation of the outgoing face moments of the angular flux via the characteristic relation, the source moments and expansion coefficients over the cell must be transformed into the CT coordinate system. In accordance with Eq. 2.14, the moments and expansion coefficients for the source distribution in the cell and CT coordinate systems are related via

$$\mathbf{S} = \boldsymbol{M}\mathbf{s} \tag{2.16}$$

and

$$\mathbf{S}^v = \boldsymbol{M}^v\mathbf{s}^v \tag{2.17}$$

respectively, where the v superscript implies CT coordinate system, and the $\vec{i}^{th}$ elements of $\mathbf{s}$ and $\mathbf{s}^v$ are $s_{\vec{i}}$ and $s^v_{\vec{i}}$, respectively, with analogous relationships for the moment vectors $\mathbf{S}$ and $\mathbf{S}^v$. The distributed source within a CT is equal to the cell source distribution over the volume of the tetrahedron with respect to the global coordinate system, $S(\vec{r}) = S^v(\vec{r})$, where S^v is the distributed source over the volume of the CT. Thus, the spatial moments of the source over the CT are obtained by integrating the product of the corresponding monomial and the cell distributed source over the domain of the CT, i.e.,

$$S^v_{\vec{i}} = \frac{1}{V^v}\int_{V^v} dV^v B^v_{\vec{i}}(\vec{r})S(\vec{r}) \tag{2.18}$$

Since the distributed source moments are expressed in the cell coordinate system, Eq. 2.18 must reflect this coordinate transformation. Substituting Eq. 2.13, with $g(\vec{u}) = S(\vec{u})$, into Eq. 2.18 and evaluating the expression in the CT coordinate system yields the following relation between the CT source moments, $\mathbf{S}^v$, and the cell source expansion coefficients, $\mathbf{s}$,

$$\mathbf{S}^v = \boldsymbol{P}\mathbf{s} \tag{2.19}$$

where matrix $\boldsymbol{P}$ contains the basis product integration. This matrix allows the transformation of the distributed source expressed via expansion coefficients over a cell into a source distribution expressed via CT moments over a CT. However, the explicit evaluation of the matrix $\boldsymbol{P}$ requires careful consideration. The cell moments of the distributed source are expressed in the cell coordinate system, while the CT moments of the distributed source are expressed in the CT coordinate system. In order to correctly evaluate matrix $\boldsymbol{P}$, the integration must be performed in the CT coordinate system and the source expansion coefficients in the cell coordinate system must be transformed into the CT coordinate system.

In order to derive the characteristic equation, and determine the outgoing face angular fluxes, two more procedures are required. First, the upstream cell's outgoing face angular flux moments from a neighboring cell must be transformed into downstream incoming face moments. Second, it is necessary to transform the incoming face angular flux moments into CT face angular moments. Once these procedures are applied to the specified moments, the characteristic relation can be derived in the CT coordinate system.

2.2.3 Upstream to Downstream Face Angular Flux Moment Transformation

Analogous to the source distribution, the upstream/downstream face angular flux moments, denoted by the vectors $\boldsymbol{\Psi}^{F,up/down}$, and the expansion coefficients, denoted by the vector $\boldsymbol{\psi}^{F,up/down}$, are related via,

$$\boldsymbol{\Psi}^{F,up} = \boldsymbol{M}^F \boldsymbol{\psi}^{F,up} \tag{2.20}$$

$$\boldsymbol{\Psi}^{F,down} = \boldsymbol{M}^F \boldsymbol{\psi}^{F,down} \tag{2.21}$$

where the $\vec{i}^{th}$ element of each of these vectors corresponds to the $\vec{i}^{th}$ moment and $\vec{i}^{th}$ expansion coefficient, respectively, of the corresponding quantity. The matrix $\boldsymbol{M}^F$ is defined in analogy to Eq. 2.15

$$\boldsymbol{M}^F \equiv 2 \int_0^1 du_1^F \int_0^{u_1^F} du_2^F B_{\vec{i}^F}^F B_{\vec{i}^F}^{F\,\boldsymbol{T}} \tag{2.22}$$

where $\vec{i}^F = \{i_1^F, i_2^F\}$ and the components of this vector satisfy either $0 \leq i_1^F + i_2^F \leq \Lambda'$ or $0 \leq i_1^F + i_2^F \leq 2\Lambda$, depending on the expansion method. In order to relate the upstream and downstream moments, which may not be expressed in the same face coordinate system, we assume that the angular flux evaluated on a given face in the global coordinate system is continuous across that face, i.e. no jump conditions on cell interfaces, $\psi^{F,up}(\vec{r}) = \psi^{F,down}(\vec{r})$, such that $\vec{r}$ is a point on the face separating the indicated tetrahedra. Thus, the spatial moments of the downstream face angular flux become

$$\Psi_{\vec{i}^F}^{F,down} = \frac{1}{A^F} \int_{A^F} dA^F B_{\vec{i}^F}^{F,down}(\vec{r}) \psi^{F,up}(\vec{r}) \tag{2.23}$$

Since the upstream face moments are expressed in the cell face coordinate system, Eq. 2.23 must reflect this coordinate transformation. Substituting Eq. 2.13, with $g(\vec{u}) = \psi^{F,up}(\vec{u})$ and $B_{\vec{i}}(\vec{u}) = B_{\vec{i}^F}^{F,down}(\vec{u})$, into Eq. 2.23 yields the following relation between the moments, as evaluated in the downstream cell face coordinate system

$$\boldsymbol{\Psi}^{F,down} = \boldsymbol{T} \boldsymbol{\Psi}^{F,up} \tag{2.24}$$

where matrix $\boldsymbol{T}$ contains elements representing the basis product integration. This matrix allows the transformation of upstream face moments in the upstream coordinates system into downstream moments in the downstream coordinate system.

2.2.4 Incoming Angular Flux Cell and CT Transformation

In order to apply the characteristic relation, an additional transformation is introduced to map the incoming angular flux moments from the cell face coordinate system to the CT face coordinate system. The development of this transformation is rather similar to the development of the transformation of the distributed source. The incoming face angular flux moments and expansion coefficients over the cell and CT, respectively, are related via the following expressions,

$$\boldsymbol{\Psi}^{F,in} = \boldsymbol{M}^{F}\boldsymbol{\psi}^{F,in} \tag{2.25}$$

$$\boldsymbol{\Psi}^{f,in} = \boldsymbol{M}^{f}\boldsymbol{\psi}^{f,in} \tag{2.26}$$

where $\boldsymbol{M}^{f}$ is defined in a similar manner to Eq. 2.22

$$\boldsymbol{M}^{f} \equiv 2\int_{0}^{1} dq_1^f \int_{0}^{q_1^f} dq_2^f B_{\vec{i}^f}^f B_{\vec{i}^f}^{f\,\boldsymbol{T}} \tag{2.27}$$

where $\vec{i}^f = \{i_1^f, i_2^f\}$ and the components of this vector satisfy either $0 \leq i_1^f + i_2^f \leq \Lambda'$ or $0 \leq i_1^f + i_2^f \leq 2\Lambda$, depending on the expansion method. Again we assume no jump conditions on tetrahedron faces so that in the global coordinate system we may write $\psi^{f,in}(\vec{r}) = \psi^{F,in}(\vec{r})$. The spatial moments of the CT incoming face angular flux in terms of the *cell* face incoming angular flux expansion, are expressed by the following relation

$$\Psi_{\vec{i}^f}^{f,in} = \frac{1}{A^f}\int_{A^f} dA^f B_{\vec{i}^f}^{f,in}(\vec{r})\psi^{F,in}(\vec{r}) \tag{2.28}$$

Substituting the explicit expansion for $\psi^{F,in}(\vec{r})$ in the cell face coordinate system into Eq. 2.28 yields the following relation between the moments written in vector form, with the elements interpreted as before,

$$\boldsymbol{\Psi}^{f,in} = \boldsymbol{p}^{F}\boldsymbol{\Psi}^{F,in} \tag{2.29}$$

where matrix $\boldsymbol{p}^{F}$ contains the basis product integration element by element. This matrix allows the transformation of incoming face moments in the cell coordinate system into incoming moments in the CT coordinate system.

2.2.5 Face Moments of the Arbitrary-Order Characteristic Relation

The outgoing angular face flux for a CT, assuming known incoming and distributed source spatial moments in the CT coordinate system, can be computed using the characteristic relation. The characteristic relation originates from the exact local inversion of the streaming-plus-collision operator of the transport equation

along the angular direction. The general characteristic relation in the CT coordinate system for the case of isotropic fixed source is

$$\psi^v(\vec{r}^{in} + t\hat{\Omega}) = \psi^{f,in}(\vec{r}^{in})e^{-\sigma_T t} + \int_0^t dt' S^v(\vec{r}^{in} + t'\hat{\Omega})e^{-\sigma_T(t-t')}, 0 \leq t \leq \tau, \tag{2.30}$$

where t is the physical distance measured along the characteristic from the incoming point $\vec{r}^{in}$, τ is the physical extent of the cell along $\hat{\Omega}$, and the superscript v denotes the selected CT domain within the cell. Evaluating Eq. 2.30 on the outgoing face of the CT then taking moments in the CT coordinate system yields

$$\mathbf{\Psi}_{\vec{i}^f}^{f,out} = \frac{1}{A^f}\int_{A^f} dA^f B_{\vec{i}^F}^{F,out}\psi^{f,out}(\vec{r}) \tag{2.31}$$

from which moments on the cell's outgoing face, in the cell coordinate system, are accumulated via

$$\mathbf{\Psi}_{\vec{i}^F}^{F,out} = \sum_f \frac{A^f}{A^F}\mathbf{\Psi}_{\vec{i}^f}^{f,out} \tag{2.32}$$

Recalling Eqs. 2.26 and 2.17, the following expression for the outgoing CT face moments is obtained

$$\mathbf{\Psi}_{\vec{i}^f}^{f,out} = \boldsymbol{F}\boldsymbol{\psi}^{f,in} + \boldsymbol{V}\mathbf{s}^v \tag{2.33}$$

where the elements of matrices $\boldsymbol{F}$ and $\boldsymbol{V}$ represent the integration of the exponential functions and basis product in the CT coordinate system, and the elements of the vectors $\boldsymbol{\psi}^{f,in}$ and $\mathbf{s}^v$ are $\psi_{\vec{i}}^{f,in}$ and $s_{\vec{i}}^v$, respectively.

2.2.6 Incoming and Outgoing Angular Flux Cell Transformation

Once the outgoing face moments in the cell face coordinate system are computed, they must be transformed into the cell coordinate system via the relation,

$$\mathbf{\Psi}^F = \boldsymbol{T}^F\boldsymbol{\psi}^F \tag{2.34}$$

where the matrix $\boldsymbol{T}^F$ contains the basis product integration. Note that the evaluation of $B_{\vec{i}}(\vec{u})$ will depend on the face under consideration.

2.2.7 The Arbitrary Order Characteristic Relation

Given a known distributed source and incoming face angular flux, the spatial moments of the angular flux over the CT can be computed via the characteristic relation. As shown in the previous section, the characteristic relation exactly satisfies the arbitrary order balance equation. Thus, the spatial moments computed from either equation will comprise the same solution. However, due to the fact that finite arithmetic precision can be affected by the buildup of round-off error, two equivalent mathematical statements may yield either slightly or significantly different results. In the case of the spatial moments of the angular flux, rather large discrepancies were observed as the cells were made less absorbing. Conversely, in the case of highly

absorbing cells, the discrepancies between the results obtained via the characteristic and the balance equations formulations diminished, hence it was possible to verify numerically the equivalence between the two formulations.

In this section the procedure for computing the spatial moments of the angular flux from the characteristic equation is reviewed and all relevant relations are derived. Recall that in the CT coordinate system, the characteristic relation is given by Eq. 2.30. Instead of obtaining the spatial moments in the CT coordinate system, the moments in the *cell* coordinate system will be directly obtained from the characteristic equation,

$$\mathbf{\Psi} = \sum_{v} \left(\frac{V^v}{V} \right) \mathbf{\Psi}^v \tag{2.35}$$

where the $\vec{i}^{th}$ element of the vector $\mathbf{\Psi}^v$ is computed by,

$$\begin{aligned} \psi^v_{\vec{i}} &= \frac{1}{V^v} \int_{V^v} dV^v B_{\vec{i}}(\vec{r}) \psi^v(\vec{r}) \\ &= 6 \int_0^1 dq_1 \int_0^{q_1} dq_2 \int_0^{q_2} dq_3 B_{\vec{i}}(\vec{u}) \psi^v(\vec{q}) \end{aligned} \tag{2.36}$$

By substituting Eq. 2.30 into Eq. 2.36, the following expression for the CT spatial moments is obtained,

$$\mathbf{\Psi}^v = \boldsymbol{F}^v \boldsymbol{\psi}^{f,in} + \boldsymbol{V}^v \mathbf{s}^v \tag{2.37}$$

Note that the basis multiplying the characteristic equation is in the cell coordinate system. This concludes the introduction and development of the necessary equations and relations needed to apply the AHOT-C formalism to unstructured tetrahedral grids. The only outstanding issue that remains unresolved is the explicit computation of the integral kernels. In the next section the evaluation of these integral kernels will be discussed and series expansions will be derived in order to obtain stable expressions suitable for computing the spatial moments as the cells become optically thin.

2.3 Series Expansion of Integral Kernels in Arbitrary-Order Characteristics Relation

The expressions derived for the CT, that relate the outgoing face-moments and cell volume-moments of the angular flux via the characteristic relation, can be evaluated analytically by repeatedly applying integration by parts to the basis functions.

In order to derive the series expressions for the outgoing face moments of the angular flux, the exponential function appearing in the integrand is expanded locally into a Taylor series,

$$e^{-\epsilon q_2^f} = \sum_{n=0}^{\infty} \frac{(-1)^n}{n!} \epsilon^n \left(q_2^f \right)^n \tag{2.38}$$

then substituted into the integral expression to yield,

$$\Gamma_{\gamma_1^f,\gamma_2^f}(\epsilon) = \sum_{n=0}^{\infty} \frac{(-1)^n}{n!} \frac{\epsilon^n}{(\gamma_1^f + \gamma_2^f + n + 2)(\gamma_2^f + n + 1)} \tag{2.39}$$

In a similar development, the exponential function in the cell volume is split into the product of two exponentials, where the first term has the Taylor expansion Eq. 2.38, and the second term yields,

$$e^{\epsilon q_2^f} = \sum_{n=0}^{\infty} \frac{1}{n!} \left(q_2^f\right)^n \tag{2.40}$$

These two Taylor expansions are then substituted into the corresponding integral expression in order to obtain the following series representation,

$$\Gamma_{\gamma_1,\gamma_2,\gamma_3}(\epsilon) = \sum_{n=0}^{\infty} \sum_{m=0}^{\infty} \frac{(-1)^m \epsilon^{n+m}}{n!m!} \frac{1}{(\gamma_1 + \gamma_2 + \gamma_3 + n + m + 3)(\gamma_2 + \gamma_3 + n + m + 2)(\gamma_3 + n + 1)} \tag{2.41}$$

In order to derive the series expressions for the spatial moment integrals of the angular flux over the cell volume, the exponential function for the incoming face angular fluxes for the the spatial moments over the volume is expanded into a polynomial series in a similar fashion to the previous procedure,

$$e^{-\epsilon q_3^f} = \sum_{n=0}^{\infty} \frac{(-1)^n}{n!} \epsilon^n \left(q_3\right)^n \tag{2.42}$$

that is then substituted into the corresponding integral relation in order to obtain the following expressions,

$$\Gamma^v_{\gamma_1,\gamma_2,\gamma_3}(\epsilon) = \sum_{n=0}^{\infty} \frac{(-1)^n \epsilon^n}{n!} \frac{1}{(\gamma_1 + \gamma_2 + \gamma_3 + n + 3)(\gamma_2 + \gamma_3 + n + 2)(\gamma_3 + n + 1)} \tag{2.43}$$

$$\begin{aligned}\Gamma^v_{\gamma_1,\gamma_2,\gamma_3,\gamma_3'}(\epsilon) = \sum_{n=0}^{\infty} \sum_{m=0}^{\infty} \frac{(-1)^m \epsilon^{n+m}}{n!m!} &\frac{1}{(\gamma_1 + \gamma_2 + \gamma_3 + \gamma_3' + n + m + 4)} \\ &\times \frac{1}{(\gamma_2 + \gamma_3 + \gamma_3' + n + m + 3)(\gamma_3 + \gamma_3' + n + m + 2)(\gamma_3' + n + 1)}\end{aligned} \tag{2.44}$$

In summary, the integral kernels contained in the arbitrary-order characteristic equations were expanded using a Taylor series of the exponential functions and their corresponding integrals were evaluated on a term by term basis. These integral kernels, that are now represented by local series expansions, enable computing the contribution of the incoming angular fluxes and distributed source to the outgoing face moments and spatial moments of the angular flux over the given cell. It is important to note that this local expansion treatment resolves previously reported instabilities of the computational method in the limit of thin cell and with increasing spatial approximation order [5]. Evidence to this statement is provided by numerical experiments that were reported elsewhere.

This concludes the development of a robust AHOT-C-UG methodology for the solution to the discrete-ordinates approximation to the transport equation on three dimensional tetrahedral grids.

3. Adjoint Theory

3.1 Adjoint Basics

The forward steady state neutron transport equation with an external source (implicitly not super-critical by lack of time dependence) is:

$$\mathbf{M}\psi = Q, \qquad \vec{r} \in V,\, \hat{\Omega} \in 4\pi,\, 0 < E < \infty \tag{3.1}$$

with boundary conditions

$$\psi = \psi^b, \qquad \vec{r} \in \partial V,\, \hat{\Omega}\cdot\hat{n} < 0,\, 0 < E < \infty \tag{3.2}$$

Where $\mathbf{M} = \mathbf{S} - \mathbf{F}$ and:

$$\mathbf{S}\psi = \hat{\Omega}\cdot\nabla\psi(\vec{r},\hat{\Omega},E) + \Sigma_t(\vec{r},E)\psi(\vec{r},\hat{\Omega},E) - \int_0^\infty\int_{4\pi}\Sigma_s(\vec{r},E'\rightarrow E,\hat{\Omega}'\cdot\hat{\Omega})\psi(\vec{r},\hat{\Omega}',E')\,d\hat{\Omega}'\,dE' \tag{3.3}$$

$$\mathbf{F}\psi = \frac{\chi(\vec{r},E)}{4\pi}\int_0^\infty\int_{4\pi}\nu\Sigma_f(\vec{r},E')\psi(\vec{r},\hat{\Omega}',E')\,d\hat{\Omega}'\,dE' \tag{3.4}$$

We now define an inner product of two functions as:

$$(f,g) = \int_0^\infty\int_{4\pi}\int_V f(\vec{r},\hat{\Omega},E)g(\vec{r},\hat{\Omega},E)\,dV\,d\hat{\Omega}\,dE \tag{3.5}$$

So then

$$\begin{aligned}(f,\mathbf{M}g) = \int_0^\infty\int_{4\pi}\int_V f(\vec{r},\hat{\Omega},E)\Big[&\hat{\Omega}\cdot\nabla g(\vec{r},\hat{\Omega},E) + \Sigma_t(\vec{r},E)g(\vec{r},\hat{\Omega},E)\\ &- \int_0^\infty\int_{4\pi}\Sigma_s(\vec{r},E'\rightarrow E,\hat{\Omega}'\cdot\hat{\Omega})g(\vec{r},\hat{\Omega}',E')\,d\hat{\Omega}'\,dE'\\ &- \frac{\chi(\vec{r},E)}{4\pi}\int_0^\infty\int_{4\pi}\nu\Sigma_f(\vec{r},E')g(\vec{r},\hat{\Omega}',E')\,d\hat{\Omega}'\,dE'\Big]\,dV\,d\hat{\Omega}\,dE\end{aligned} \tag{3.6}$$

Using the divergence theorem and some algebraic manipulation we can get:

$$\begin{aligned}(f,\mathbf{M}g) = \int_0^\infty\int_{4\pi}\int_V\Big[&-\hat{\Omega}\cdot\nabla f(\vec{r},\hat{\Omega},E) + \Sigma_t(\vec{r},E)f(\vec{r},\hat{\Omega},E) - \int_0^\infty\int_{4\pi}\Sigma_s(\vec{r},E\rightarrow E',\hat{\Omega}\cdot\hat{\Omega}')f(\vec{r},\hat{\Omega}',E')\,d\hat{\Omega}'\,dE'\\ &- \frac{\nu\Sigma_f(\vec{r},E)}{4\pi}\int_0^\infty\int_{4\pi}\chi(\vec{r},E')f(\vec{r},\hat{\Omega},E)\,d\hat{\Omega}'\,dE'\Big]g(\vec{r},\hat{\Omega}',E')\,dV\,d\hat{\Omega}\,dE\\ &+ \int_0^\infty\int_{4\pi}\int_{\partial V}(\hat{\Omega}\cdot\hat{n})f(\vec{r},\hat{\Omega},E)g(\vec{r},\hat{\Omega},E)\,dS\,d\hat{\Omega}\,dE\end{aligned} \tag{3.7}$$

Then if we define the adjoint operator, $\mathbf{M}^*$, as:

$$\mathbf{M}^*\psi = -\hat{\Omega}\cdot\nabla\psi(\vec{r},\hat{\Omega},E) + \Sigma_t(\vec{r},E)\psi(\vec{r},\hat{\Omega},E) - \int_0^\infty\int_{4\pi}\Sigma_s(\vec{r},E\to E',\hat{\Omega}\cdot\hat{\Omega}')\psi(\vec{r},\hat{\Omega}',E')\,d\hat{\Omega}'\,dE' - \frac{\nu\Sigma_f(\vec{r},E)}{4\pi}\int_0^\infty\int_{4\pi}\chi(\vec{r},E')\psi(\vec{r},\hat{\Omega}',E')\,d\hat{\Omega}'\,dE' \quad (3.8)$$

Investigating the surface integral at the end of the adjoint operator, we can split it up to get:

$$\int_0^\infty\int_{4\pi}\int_{\partial V}(\hat{\Omega}\cdot\hat{n})f(\vec{r},\hat{\Omega},E)g(\vec{r},\hat{\Omega},E)\,dS\,d\hat{\Omega}\,dE = \int_0^\infty\int_{\partial V}\int_{\hat{\Omega}\cdot\hat{n}>0}(\hat{\Omega}\cdot\hat{n})f(\vec{r},\hat{\Omega},E)g(\vec{r},\hat{\Omega},E)\,d\hat{\Omega}\,dS\,dE - \int_0^\infty\int_{\partial V}\int_{\hat{\Omega}\cdot\hat{n}<0}\left|\hat{\Omega}\cdot\hat{n}\right|f(\vec{r},\hat{\Omega},E)g(\vec{r},\hat{\Omega},E)\,d\hat{\Omega}\,dS\,dE \quad (3.9)$$

Then it can be observed that:

$$(f,\mathbf{M}g) + \int_0^\infty\int_{\partial V}\int_{\hat{\Omega}\cdot\hat{n}<0}\left|\hat{\Omega}\cdot\hat{n}\right|f(\vec{r},\hat{\Omega},E)g(\vec{r},\hat{\Omega},E)\,dS\,d\hat{\Omega}\,dE = (\mathbf{M}^*f,g) + \int_0^\infty\int_{\partial V}\int_{\hat{\Omega}\cdot\hat{n}>0}(\hat{\Omega}\cdot\hat{n})f(\vec{r},\hat{\Omega},E)g(\vec{r},\hat{\Omega},E)\,dS\,d\hat{\Omega}\,dE \quad (3.10)$$

So if we carefully define the adjoint problem as:

$$\mathbf{M}^*\psi^* = Q^*, \qquad \vec{r}\in V,\ \hat{\Omega}\in 4\pi,\ 0<E<\infty \quad (3.11)$$

with boundary conditions

$$\psi^* = \psi^{*b}, \qquad \vec{r}\in\partial V,\ \hat{\Omega}\cdot\hat{n}>0,\ 0<E<\infty \quad (3.12)$$

Then recalling the forward transport problem, we can get:

$$(\psi^*,Q) + \int_0^\infty\int_{\partial V}\int_{\hat{\Omega}\cdot\hat{n}<0}\left|\hat{\Omega}\cdot\hat{n}\right|\psi^*(\vec{r},\hat{\Omega},E)\psi^b(\vec{r},\hat{\Omega},E)\,dS\,d\hat{\Omega}\,dE = (Q^*,\psi) + \int_0^\infty\int_{\partial V}\int_{\hat{\Omega}\cdot\hat{n}>0}(\hat{\Omega}\cdot\hat{n})\psi^{*b}(\vec{r},\hat{\Omega},E)\psi(\vec{r},\hat{\Omega},E)\,dS\,d\hat{\Omega}\,dE \quad (3.13)$$

Q^* is often referred to as a "response" function. Indeed, if we consider some detector region V_d with response cross section $\Sigma_d(\vec{r},E)$, then if we setup our forward and adjoint problems as:

$$\mathbf{M}\psi = Q; \qquad \psi^b = 0; \qquad \mathbf{M}^*\psi^* = Q^* = \zeta_d(\vec{r})\Sigma_d(\vec{r},E); \qquad \psi^{*b} = 0 \quad (3.14)$$

Where

$$\zeta_d(\vec{r}) = \begin{cases} 1 & \vec{r}\in V_d \\ 0 & \vec{r}\notin V_d \end{cases} \quad (3.15)$$

So we can see then that the detector response R can be expressed as:

$$R = (\psi,\zeta_d\Sigma_d) = (\psi,Q^*) = (Q,\psi^*) \quad (3.16)$$

So we can see that the adjoint flux describes the importance of the source in the detector response.

Various choices of response functions and adjoint boundary conditions can lead to various physical interpretations. As shown, a non-zero response function and adjoint boundary conditions lead to interpretation of

the adjoint flux as importance weight of the source and incident boundary flux on the detector response. Analogously, a zero response function and non-zero adjoint boundary condition can lead to interpretation of the adjoint flux as the contribution to leakage across a boundary surface for the source and incident boundary flux.

These interpretations are for basic physical choices of response functions and adjoint boundary conditions. If the choices are more complex, then the intuitive interpretations for the meaning of the adjoint flux can break down.

Similarly, for $k-$eigenvalue problems:

$$\mathbf{S}\psi = \frac{1}{k}\mathbf{F}\psi; \qquad \psi^b = 0 \tag{3.17}$$

Then the adjoint problem is defined:

$$\mathbf{S}^*\psi^* = \frac{1}{k^*}\mathbf{F}^*\psi^*; \qquad \psi^{*b} = 0 \tag{3.18}$$

Where $\mathbf{S}^*$ and $\mathbf{F}^*$ are intuitively defined based on the separation of $\mathbf{M}$ into $\mathbf{S}$ and $-\mathbf{F}$, so that in the same way $\mathbf{M}^*$ is separated into $\mathbf{S}^*$ and $-\mathbf{F}^*$ (this can formally be derived as well if so desired). So that:

$$(\psi^*, \mathbf{S}\psi) = (\mathbf{S}^*\psi^*, \psi) = \left(\psi^*, \frac{1}{k}\mathbf{F}\psi\right) = \left(\frac{1}{k^*}\mathbf{F}^*\psi^*, \psi\right) \tag{3.19}$$

And it can be shown that $k^* = k$, which is to say the eigenvalue is self adjoint.

The adjoint equation and these relations then serve as the basis for perturbation theory.

3.2 THOR Adjoint

With the basics of the adjoint equation stated, we can now investigate methods of calculating the adjoint using traditional transport methods. Notice that for the case with vacuum or reflective boundary conditions, nothing need be changed between the transport and adjoint equations except that the transport operator be transposed. It should also be noticed that a fixed source problem where an adjoint is computed has the source being defined as the response function.

The one caveat with the solution change is that the angles are reversed for the flux due to the difference in the boundary conditions (even for zero or reflective boundary conditions). As such, the flux computed from a transposed adjoint problem needs an additional correction to become the true adjoint solution. This correction involves assigning flux to the opposite angle than the one it was previously in. Consider the multigroup transposed transport equation (not adjoint):

$$M^T\psi^\dagger = Q \tag{3.20}$$

Then M^T is equal to the adjoint operator, but with traditional boundary conditions. To account for this we make the change:

$$\psi^\dagger(\hat{\Omega}) = \psi^*(-\hat{\Omega}) \tag{3.21}$$

Note that these observations only hold for a symmetric quadrature where for any quadrature angle $\hat{\Omega}_m$, $\hat{\Omega}_n = -\hat{\Omega}_m$ also exists on the quadrature set.

The primary impact this has is on angular moments of the flux. The 0th moment, or scalar flux, does not change since:

$$\sum_m \psi^*(\hat{\Omega}_m) = \sum_m \psi^*(-\hat{\Omega}_m) \tag{3.22}$$

In fact, all even moments will not change since an even basis function maintains the property $b_{even}(\hat{\Omega}) = b_{even}(-\hat{\Omega})$. So it can be seen that for even moments, we get:

$$\sum_m b_{even}(\hat{\Omega})\psi^*(\hat{\Omega}_m) = \sum_m b_{even}(-\hat{\Omega})\psi^*(\hat{\Omega}_m) = \sum_m b_{even}(\hat{\Omega})\psi^*(-\hat{\Omega}_m) \tag{3.23}$$

However, odd moments will become negative since the odd basis functions have the property $b_{odd}(\hat{\Omega}) = -b_{odd}(-\hat{\Omega})$. So it can be seen that for odd moments, we get:

$$\sum_m b_{odd}(\hat{\Omega})\psi^*(\hat{\Omega}_m) = -\sum_m b_{odd}(-\hat{\Omega})\psi^*(\hat{\Omega}_m) = -\sum_m b_{odd}(\hat{\Omega})\psi^*(-\hat{\Omega}_m) \tag{3.24}$$

Bibliography

[1] M. L. Adams. Discontinuous finite element solutions in thick diffusive problems. *Nuclear Science and Engineering*, 137:298–333, 2001.

[2] M. L. Adams, T. A. Wareing, and W. F. Walters. Characteristic methods in thick diffusive problems. *Nuclear Science and Engineering*, 130:1846, 1998.

[3] Y. Y. Azmy. Comparison of three approximations to the linear-linear nodal transport method in weighted diamond-difference form. *Nuclear Science and Engineering*, 100:190, 1988.

[4] Y. Y. Azmy. The weighted diamond difference form of nodal transport methods. *Nuclear Science and Engineering*, 98:29, 1988.

[5] Y. Y. Azmy and A. Barnett. Arbitrarily high order transport method of the characteristic type in unstructured grids. International Topical Meeting on Mathematical Methods for Nuclear Applications, American Nuclear Society, 2001.

[6] Yousry Y. Azmy. Arbitrarily high order characteristic methods for solving the neutron transport equation. *Annals of Nuclear Energy*, 19:593–606, 1992.

[7] C. R. Brennan, R. L. Miller, and K. A. Mathews. Split-cell exponential characteristic transport method for unstructured tetrahedral meshes. *Nuclear Science and Engineering*, 138:2644, 2001.

[8] M. D. DeHart, R. E. Pevey, and T. A. Parish. An extended step characteristic method for solving the transport equation in general geometries. *Nuclear Science and Engineering*, 118:7990, 1994.

[9] J. I. Duo and Y. Y. Azmy. Spatial convergence study of discrete ordinates methods via the singular characteristic tracking algorithm. *Nuclear Science and Engineering*, 162:41, 2009.

[10] R. M. Ferrer. *An Arbitrarily High Order Transport Method of the Characteristic Type for Unstructured Tetrahedral Grids*. PhD thesis, The Pennsylvania State University, Department of Mechanical and Nuclear Engineering, 2010.

[11] R. M. Ferrer and Y. Y. Azmy. A robust arbitrarily high order transport method of the characteristic type for unstructured tetrahedral grids. International Topical Meeting on Mathematics, Computational Methods and Reactor Physics, American Nuclear Society, 2009.

[12] R. M. Ferrer and Y. Y. Azmy. A robust arbitrarily high-order transport method of the characteristic type for unstructured grids. *Nuclear Science and Engineering*, 172:33, 2012.

[13] R. E. Grove. The slice balance approach (sba): A characteristic-based, multiple balance sn approach on unstructured polyhedral meshes. Joint International Topical Meeting on Mathematics and Computations, Supercomputing, Reactor Physics and Nuclear and Biological Applications, American Nuclear Society, 2005.

[14] E. W. Larsen and R. E. Alcouffe. The linear characteristic method for spatially discretizing the discrete-ordinates equations in (x,y)-geometry. volume 1, page 99. International Topical Meeting on Advances in Mathematical Methods for the Solution of Nuclear Engineering Problems, American Nuclear Society, 1981.

[15] K. D. Lathrop. Spatial differencing of the transport equation: Positivity vs. accuracy. *Journal of Computational Physics*, 4:475498, 1969.

[16] E. E. Lewis and W. F. Miller, Jr. *Computational Methods of Neutron Transport*. American Nuclear Society, La Grange Park, Illinois, 1993.

[17] K. A. Mathews, R. L. Miller, and C. R. Brennan. Split-cell, linear characteristic transport method for unstructured tetrahedral meshes. *Nuclear Science and Engineering*, 136:178201, 2000.

[18] D. J. Miller, K. A. Mathews, and C. R. Brennan. Split-cell discrete ordinates transport on an unstructured grid of triangular cells. *Transport Theory and Statistical Physics*, 25:833, 1996.

[19] R. Sanchez and N. J. McCormick. A review of neutron transport approximations. *Nuclear Science and Engineering*, 80:481535, 1982.

[20] Sebastian Schunert and Yousry Y. Azmy. Comparison of spatial discretization methods for solving the sn equations using a three-dimensional method of manufactured solutions benchmark suite with escalating order of non-smoothness. *Nuclear Science and Engineering*, 180:1, 2015.

[21] Y. Wang and J. C. Ragusa. A high-order discontinuous galerkin method for the s_n transport equations on 2d unstructured triangular meshes. *Annals of Nuclear Energy*, 36:931939, 2009.